9th International Colloquium on Bluff Body Aerodynamics and Applications
University of Birmingham, Birmingham, UK
29th July – 2nd August 2024

On the three-dimensional coherent structures in the wake of flatback airfoils

Konstantinos Kellaris[a], George Papadakis[b], Marinos Manolesos[c]

[a]*National Technical University of Athens, Athens, Greece, kkellaris@mail.ntua.gr*
[b]*National Technical University of Athens, Athens, Greece, papis@fluid.mech.ntua.gr*
[c]*National Technical University of Athens, Athens, Greece, marinos@fluid.mech.ntua.gr*

SUMMARY
Flatback airfoils, i.e. airfoils with blunt trailing edge, are utilised at the root region of large wind turbine blades. Recently, a low-drag pocket has been identified at a high angle of attack regime, before stall and is the focus of the present study. Two angles of attack – one inside (12°) and one outside (0°) of the low-drag pocket - are examined. We use data-driven modal analysis techniques to investigate the three-dimensional coherent structures in the wake of the airfoil. Results of Detached Eddy Simulations demonstrate the drag reduction and the different three-dimensional wake coherent structures. The coherent structures are extracted via the multiscale Proper Orthogonal Decomposition method, ensuring the spatial modes of the dataset have relatively pure spectral content. The primary instability (Kármán vortex street) dominates in both cases. However, the secondary instability is distinguishable only for the 12° case and is identified as a Mode S′ instability.
Keywords: flatback airfoils, secondary wake instabilities, DES, modal analysis

1. INTRODUCTION

As wind turbine (WT) rotor diameters increase in size, aiming to lower the Levelized Cost of Energy (LCOE), flatback (FB) airfoils, i.e., airfoils with a blunt trailing edge (TE), have gained traction in recent years. FB airfoils are placed at the root of WT blades, providing several aerodynamic, structural, and aeroelastic benefits. From an aerodynamics point of view, FB airfoils can provide higher lift values due to the reduced adverse pressure gradient over the aft part of the suction side (Baker et al., 2006). In addition, their aerodynamic performance is insensitive to surface roughness compared to traditional sharp TE airfoils (Baker et al., 2006). Early studies performed on one of the first WT blades found in the literature that incorporated FB airfoils (SNL100-03) showed that blades with flatback airfoils can be up to 16% lighter than blades that use traditional airfoils without any performance penalty (Griffith and Richards, 2014). Additionally, due to the blunt TE and increased blade cross-sectional area, FB blades have increased flapwise stiffness. However, FB airfoils come with an increase in drag force (Baker et al., 2006), and consequently, several TE flow control devices have been proposed in order to improve their aerodynamic performance and decrease the associated drag penalty (Manolesos and Voutsinas, 2016; Papadakis and Manolesos, 2020).

Additionally, both in experimental (Barone et al., 2009; Manolesos and Voutsinas, 2016) and numerical (Barone et al., 2009; Manolesos and Papadakis, 2021) studies, a low drag "pocket" arises in a region of angles of attack (AoA) before stall. This study is a continuation of (Manolesos and Papadakis, 2021); we use high-fidelity numerical simulations to study the flow in the wake past a FB airfoil in order to identify the secondary instabilities that dominate it and further investigate the low drag "pocket" using state-of-the-art modal analysis techniques. The results of this work can be incorporated into a flow control framework.

2. METHODS

2.1 Computational Fluid Dynamics

The present investigation focused on the L30FB10 airfoil, i.e. an airfoil with a maximum thickness of 0.3c and a trailing edge height of 0.106c, where c is the chord length, also investigated in (Manolesos and Papadakis, 2021; Manolesos and Voutsinas, 2016; Papadakis and Manolesos, 2020). High-fidelity simulations were performed with the in-house solver MaPFlow (Papadakis, 2015) to solve the three-dimensional incompressible unsteady Navier-Stokes equations using the artificial compressibility method (Ntouras and Papadakis, 2020) and the Finite Volume discretisation. An O-type grid spanning 50 chord lengths with approximately 10 million cells was used following previous computational studies (Manolesos and Papadakis, 2021; Papadakis and Manolesos, 2020). The grid had a spanwise length of one chord, while the non-dimensional distance of the first cell from the airfoil was y^+=0.1. The airfoil was investigated at a high Reynolds number, namely Re=1.5x10^6, using the IDDES method (Spalart et al., 2006). This hybrid turbulence modelling approach blends the Spalart-Almaras RANS model with the Smagorinsky LES model. Specifically, the RANS variant of the model is employed near the airfoil, while the LES variant is employed away from the airfoil. The necessary grid layers and refinement around the airfoil (RANS region) are shown in the left panel of Figure 1, while in the right panel the low-drag pocket is demonstrated.

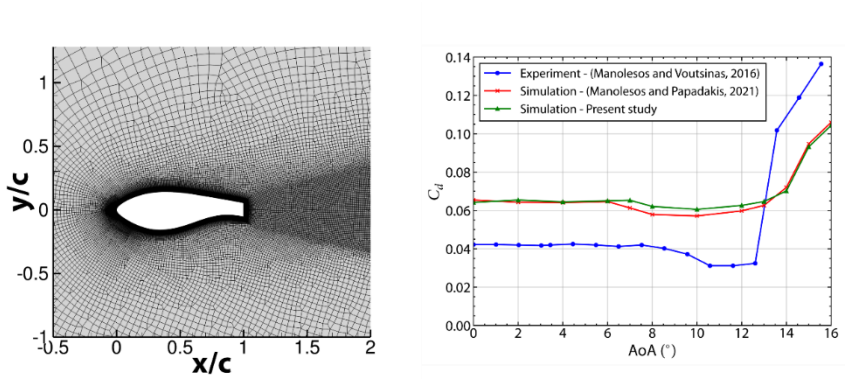

Figure 1. Left: Detail of the grid refinement layers around the airfoil. Right: The variation of the drag coefficient C_d with the angle of attack.

2.2 Modal Analysis of Wake Structures

In order to extract the three-dimensional wake coherent structures/modes, the multiscale Proper Orthogonal Decomposition (mPOD) method (Mendez et al., 2019) was utilised. At each simulation timestep, the grid data are down-sampled, using the modified Shepard's method (Shepard, 1968), into a Cartesian grid spanning one chord length at the streamwise and spanwise directions and half chord length at the y-normal direction. Afterwards, the dataset is organised into a large matrix where each column represents a timestep and each row a point in time. Then, by applying suitable band-pass filters to the temporal correlation matrix and performing POD for each filtered scale, mPOD yields a representation of the dataset modes that retain the energy optimality of the POD while simultaneously presenting more pure spectral content compared to the plain POD. For visualisation purposes, we utilise Q-criterion (Hunt et al., 1988) isosurfaces of the spatial coefficients of each mode coloured by either streamwise or spanwise vorticity. Finally, we extract the dominant frequency of each mode from the spectral behaviour of the temporal coefficients of each mode.

3. RESULTS & DISCUSSION

The difference between the vortical structures found in the two cases is demonstrated on the left panels of Figure 2 using Q-criterion isosurfaces coloured with spanwise vorticity. The wake is more organised for the 12° case, and the structure of the secondary instability observed in both cases, i.e. pairs of counterrotating vortices in the streamwise direction that connect two consecutive primary spanwise vortices, is more apparent compared to the 0° case. The primary instability dominates the first (most energetic) mPOD modes and is omitted from this abstract in the interest of brevity. Specifically, the primary instability and its harmonics appear throughout the first 10 and 6 modes for the 0° and 12° cases, respectively.

As shown in the right panels of Figure 2, the first modes that exhibit dominant spanwise behaviour are the 11th and 7th modes for the 0° and 12° cases, respectively. At 0° the associated Strouhal number (St=0.018) is an order of magnitude smaller than the one at the 12° case (St=0.106). In addition, the vortical pairs appear to be distorted along the span, an effect that is possibly introduced by the oblique shedding of the primary instability. We approximate the spanwise wavelength of the secondary instabilities, counting the number of vortex pairs along the span, leading to a spanwise wavelength of approximately 1 and 1.4 trailing edge heights at 0° and 12°, respectively.

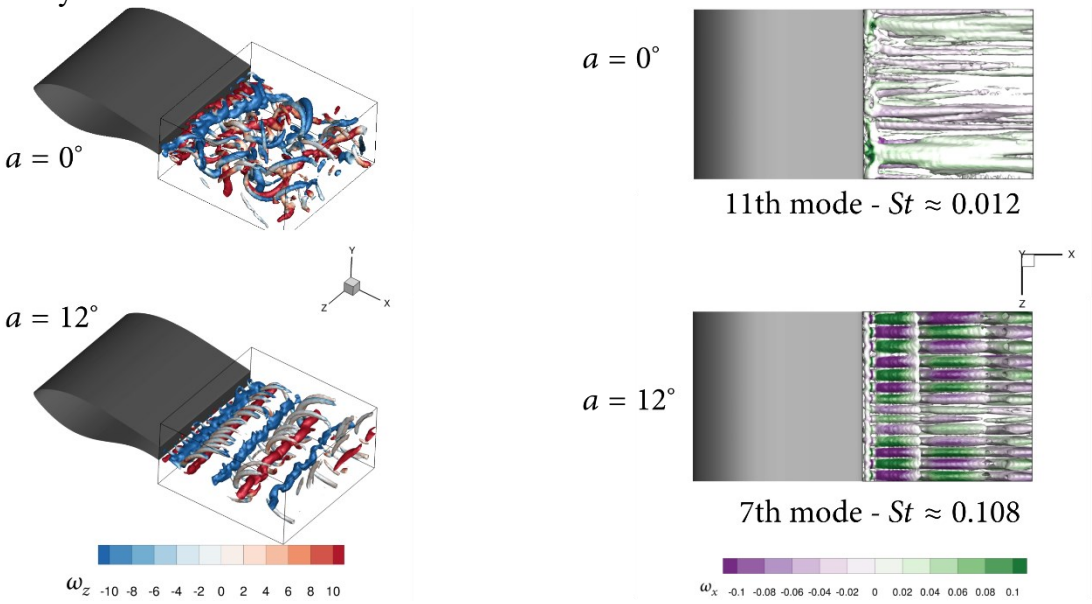

Figure 2. Q-isosurfaces coloured with vorticity. Left: Indicative snapshots at 0° (top) and 12° (bottom) coloured with spanwise vorticity. Right: The first mPOD modes exhibiting dominant spanwise behaviour at 0° (top) and 12° (bottom) coloured with streamwise vorticity.

Finally, while a comprehensive framework exists for characterising the secondary instabilities in the wake of cylindrical bluff bodies, this is not the case for elongated bluff bodies. The characterisation of the secondary instability at 0° does not correspond to a previously identified coherent mode, as the oblique shedding and the vortex dislocation significantly affect the topology of the wake. On the other hand, at 12°, the modes have a frequency that is a subharmonic of the primary instability. In addition, as shown in the bottom right panel of Figure 2, the streamwise vortical pairs' rotation direction changes at each primary vortex-shedding cycle. Therefore, the instability is characterised as the Mode S′ identified by (Ryan et al., 2005).

4. CONCLUSIONS

In summary, the three-dimensional coherent structures for the flow past a flatback airfoil were investigated for two angles of attack – one inside (12°) and one outside (0°) of the low-drag pocket. Namely, the primary instability (von Kármán vortex street) dominates the wake for the most energetic modes in both cases. However, the wake is more organised at the 12° case. The first modes demonstrating spanwise behaviour for the 0° and 12° cases are the 11^{th} and 7^{th} modes, respectively. However, the behaviour identified in these modes differs significantly for both cases. In the 12° case, the instability corresponds to the mode S′ described for the flow past elongated bluff bodies (Ryan et al., 2005), while the instability at the 0° case cannot be characterised under a preexisting framework. These new insights about the wake behaviour and organisation, in combination with the existence low-drag pocket, can potentially be used to formulate a passive drag reduction strategy based on spanwise excitation using the wavelength identified for the Mode S′ instability.

ACKNOWLEDGEMENTS

Computational resources were provided by HPC Wales, which is gratefully acknowledged. Additionally, this work was supported by computational time granted from the National Infrastructures for Research and Technology S.A. (GRNET S.A.) in the National HPC facility - ARIS - under project "HPC4FAIR" with ID pr014018_thin. Furthermore, K. Kellaris and M. Manolesos kindly acknowledge the financial support of the European project 'TWEET-IE' funded by the European Union's Horizon 2020 Research and Innovation Programme (Grant Agreement 101079125).

REFERENCES

Baker, J.P., Mayda, E.A., Van Dam, C.P., 2006. Experimental Analysis of Thick Blunt Trailing-Edge Wind Turbine Airfoils. Journal of Solar Energy Engineering 128, 422–431. https://doi.org/10.1115/1.2346701

Barone, M.F., Berg, D.E., Devenport, W.J., Burdisso, R.A., 2009. Aerodynamic and Aeroacoustic Tests of a Flatback Version of the DU97-W-300 Airfoil (No. SAND--2009-4185, 1504612). https://doi.org/10.2172/1504612

Griffith, D., Richards, P., 2014. The SNL100-03 Blade: Design Studies with Flatback Airfoils for the Sandia 100-meter Blade. (No. SAND2014-18129, 1159116, 537751). Sandia National Lab, Albuquerque, NM (United States).

Hunt, J.C.R., Wray, A.A., Moin, P., 1988. Eddies, streams, and convergence zones in turbulent flows.

Manolesos, M., Papadakis, G., 2021. Investigation of the three-dimensional flow past a flatback wind turbine airfoil at high angles of attack. Physics of Fluids 33, 085106. https://doi.org/10.1063/5.0055822

Manolesos, M., Voutsinas, S.G., 2016. Experimental study of drag-reduction devices on a flatback airfoil. AIAA Journal 54, 3382–3396. https://doi.org/10.2514/1.j054901

Mendez, M.A., Balabane, M., Buchlin, J.-M., 2019. Multi-scale proper orthogonal decomposition of complex fluid flows. Journal of Fluid Mechanics 870, 988–1036. https://doi.org/10.1017/jfm.2019.212

Ntouras, D., Papadakis, G., 2020. A coupled artificial compressibility method for free surface flows. Journal of Marine Science and Engineering 8, 590. https://doi.org/10.3390/jmse8080590

Papadakis, G., 2015. Development of a hybrid compressible vortex particle method and application to external problems including helicopter flows (PhD). National Technical University of Athens. https://doi.org/10.26240/HEAL.NTUA.1582

Papadakis, G., Manolesos, M., 2020. The flow past a flatback airfoil with flow control devices: benchmarking numerical simulations against wind tunnel data. Wind Energy Science 5, 911–927. https://doi.org/10.5194/wes-5-911-2020

Ryan, K., Thompson, M.C., Hourigan, K., 2005. Three-dimensional transition in the wake of bluff elongated cylinders. Journal of Fluid Mechanics 538, 1. https://doi.org/10.1017/s0022112005005082

Shepard, D., 1968. A two-dimensional interpolation function for irregularly-spaced data. Presented at the 23rd ACM National Conference, ACM Press, pp. 517–524. https://doi.org/10.1145/800186.810616

Spalart, P.R., Deck, S., Shur, M.L., Squires, K.D., Strelets, M.Kh., Travin, A., 2006. A New Version of Detached-eddy Simulation, Resistant to Ambiguous Grid Densities. Theoret. Comput. Fluid Dynamics 20, 181–195. https://doi.org/10.1007/s00162-006-0015-0